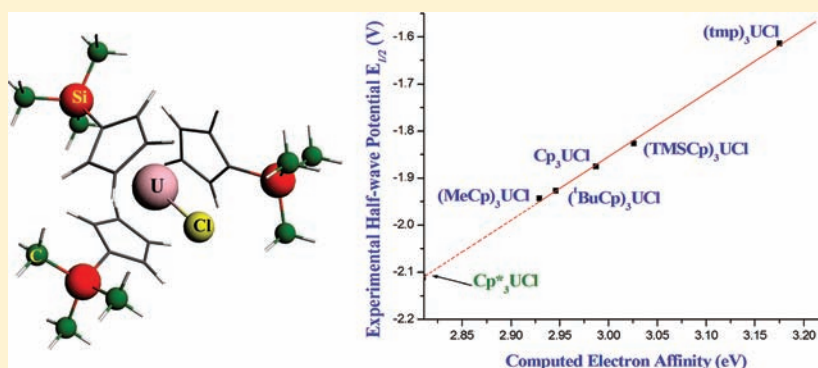


Density Functional Theory Investigation of the Redox Properties of Tricyclopentadienyl- and Phospholyuranium(IV) Chloride Complexes

Aziz Elkechai,[†] Yamina Mani,[†] Abdou Boucekkine,^{*,‡} and Michel Ephritikhine[§][†]Laboratoire de Physique et Chimie Quantique, Faculté des Sciences, Université Mouloud Mammeri de Tizi-Ouzou, 15000 Tizi-Ouzou, Algeria[‡]Institut des Sciences Chimiques de Rennes, UMR 6226 CNRS, Université de Rennes 1, Campus de Beaulieu, 35042 Rennes Cedex, France[§]CEA, IRAMIS, UMR 3299 CEA/CNRS SIS2M, CEA/Saclay, 91191 Gif-sur-Yvette, France

Supporting Information



ABSTRACT: The redox behavior of tricyclopentadienyl- and phospholyuranium(IV) chloride complexes L_3UCl with $\text{L} = \text{C}_5\text{H}_5$ (Cp), $\text{C}_5\text{H}_4\text{Me}$ (MeCp), $\text{C}_5\text{H}_4\text{SiMe}_3$ (TMSCp), $\text{C}_5\text{H}_4\text{tBu}$ (tBuCp), C_5Me_5 (Cp*), and $\text{C}_4\text{Me}_4\text{P}$ (tmp), has been investigated using relativistic density functional theory calculations, with the solvent being taken into account using the conductor-like screening model. A very good linear correlation ($r^2 = 0.99$) has been obtained between the computed electron affinities of the L_3UCl complexes and the experimental half-wave reduction potentials $E_{1/2}$ related to the $\text{U}^{\text{IV}}/\text{U}^{\text{III}}$ redox systems. From a computational point of view, our study confirms the crucial importance of spin-orbit coupling and solvent corrections and the use of an extended basis set in order to achieve the best experiment-theory agreement. Considering oxidation of the uranium(IV) complexes, the instability of the uranium(V) derivatives $[\text{L}_3\text{UCl}]^+$ is revealed, in agreement with experimental electrochemical findings. The driving roles of both the electron-donating ability of the L ligand and the U 5f orbitals on the redox properties of the complexes are brought to light. Interestingly, we found and explained the excellent correlation between variations of the uranium Hirschfeld charges following $\text{U}^{\text{IV}}/\text{U}^{\text{III}}$ electron capture and $E_{1/2}$. In addition, this work allowed one to estimate theoretically the half-wave reduction potential of $[\text{Cp}^*_3\text{UCl}]$.

INTRODUCTION

Although the chemistry of actinides has known a spectacular development during the last years, thus revealing a rich variety of molecular compounds exhibiting unique structures and reactions,^{1–5} theoretical as well as experimental studies devoted to redox processes are relatively rare. In view of their varied accessible oxidation states, a better knowledge of the redox properties of actinides is desirable, especially considering applications in the processing of spent nuclear fuels. The theoretical study of the redox properties of organometallic actinide complexes is particularly challenging because of the complexity of the computations because of relativistic effects, among them spin-orbit coupling and active 5f electrons, and the usually large size of the ligands surrounding the metal center.

Electron affinity (EA), which is the energy difference between the negative ion and the neutral species, is an important property

of atoms and molecules that has been discussed in detail in a review by Schaeffer and co-workers.⁶ The amount of experimentally determined EAs is large because Table 10 of this review⁶ presents the data concerning the EAs of 1101 species but no data relative to organometallic actinide complexes. However, such compounds, in particular those with the ubiquitous cyclopentadienyl ligand, which play a major role in many processes in homogeneous catalysis and are employed as reducing agents, deserve special attention.

The first theoretical investigation of EAs of organoactinide complexes, which was published in 2007 by the group of Kiplinger, concerned the fluoroketamide uranium(IV) complexes $[\text{Cp}^*_2\text{U}(\text{N}=\text{CMeR})_2]$ ($\text{R} = 4\text{-F-C}_6\text{H}_4$ or C_6F_5),⁷ whereas at the

Received: April 20, 2012

Published: June 5, 2012

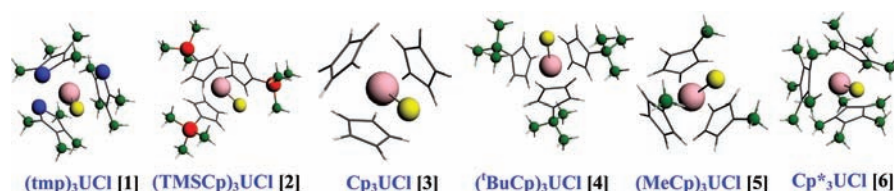


Figure 1. Studied L_3UCl complexes.

Table 1. Computed Distances (Å) and Angles (deg.) for the Uranium(III)/Uranium(IV)/Uranium(V) L_3UCl Complexes at the ZORA/BP86/TZP Level in the Gas Phase and in Solution (in Parentheses) and the Available Experimental X-ray Values for the Neutral Uranium(IV) Compounds (in Square Brackets)

ligand	U–Cl	U–L(centroid) ^a	U–C ^a	L(centroid)–U–Cl ^a
1 ^b (tmp)	2.673/2.586/2.526 (2.710/2.607/2.533) [2.670] ³⁰	2.799/2.705/2.629 (2.701/2.664/2.624) [2.61(1)]	3.111/3.018/2.957 (3.014/2.987/2.952) [2.90(8)]	99.1/97.8/98.3 (98.8/97.6/98.0) [94.8(7)]
2 (TMSCp)	2.720/2.609/2.535 (2.735/2.680/2.539)	2.544/2.512/2.478 (2.536/2.503/2.473)	2.810/2.790/2.758 (2.811/2.781/2.754)	100.8/100.4/100.7 (101.0/100.3/100.9)
3 (Cp)	2.725/2.615/2.521 (2.777/2.655/2.541) [2.559] ³²	2.521/2.496/2.472 (2.521/2.491/2.462)	2.795/2.774/2.751 (2.796/2.769/2.743) [2.740]	101.0/100.1/100.6 (101.4/99.9/100.6) [101.0]
4 (tBuCp)	2.732/2.613/2.532 (2.773/2.654/2.541)	2.572/2.529/2.501 (2.565/2.544/2.494)	2.842/2.803/2.777 (2.836/2.816/2.770)	101.2/100.2/100.2 (101.2/100.3/100.5)
5 (MeCp)	2.727/2.606/2.522 (2.749/2.628/2.536)	2.540/2.500/2.471 (2.529/2.494/2.464)	2.814/2.777/2.751 (2.804/2.771/2.745)	102.2/100.4/101.0 (102.2/100.4/101.3)
6 (Cp*)	2.703/2.600/2.545 (2.777/2.647/2.557) [2.902] ³⁴	2.704/2.644/2.575 (2.666/2.609/2.570) [2.551]	2.963/2.909/2.847 (2.929/2.874/2.849) [2.833]	97.8/96.2/96.9 (98.0/96.9/96.8) [96.2]

^aAverage values. ^bU–P^a = 2.993/3.037/2.899 (2.941/2.996/2.898) [2.927(4)]; P–C^a = 1.789/1.791/1.791 (1.789/1.790/1.792) [1.74(1)]; C–P–C^a = 90.3/90.1/90.5 (90.5/90.4/90.4) [90.10].

experimental level, some electrochemical studies of the U^{III}/U^{IV}, U^{IV}/U^V, and U^V/U^{VI} redox systems of bi- and tricyclopentadienyl- and bis(pentamethyl)cyclopentadienyluranium complexes have been carried out.^{8–14}

For our part, we investigated theoretically using relativistic density functional theory (DFT) computations and experimentally the electrochemical behavior of different series of complexes of the general formula $[Cp^*_2UX_2]$ [$X_2 = (BH_4)_2$, $(NEt_2)Cl$, Me_2 , and $(OEt)_2$],¹⁵ $[L_2U(BH_4)_2]$ [$L_2 = Cp_2$, $(tBuCp)_2$, $(tmp)_2$, $(Cp^*)_2$], and Cp^*_2 where $tmp = C_4(Me)_4P$,¹⁶ and $[Cp_3UX]$ ($X = Cl, BH_4, SPh, S^iPr$, and O^iPr).¹⁷ We found a good correlation between the DFT-computed EAs and experimental half-wave reduction potentials and confirmed that EA is directly related to the electron-donating or -withdrawing ability of the different ligands. It seemed to us interesting to extend these studies to an important class of uranium complexes, i.e., tricyclopentadienyl- and phospholyuranium(IV) complexes $[L_3UCl]$ (Figure 1), which are precursors of a large series of organouranium derivatives. More precisely, we plan to carry out a relativistic DFT investigation of the redox behavior of neutral $[(C_5H_4R)_3UCl]$ ($R = H, Me, SiMe_3$, and tBu), $[(tmp)_3UCl]$, and $[Cp^*_3UCl]$ complexes, considering not only their reduction to the corresponding uranium(III) anionic complexes but also, for a first time, their oxidation to uranium(V) cationic species. In particular, we shall investigate what the structural and electronic factors are that drive the EA and ionization potential of the uranium(IV) complexes under consideration.

COMPUTATIONAL DETAILS

Relativistic DFT¹⁸ studies based on the zeroth-order regular approximation (ZORA)¹⁹ to the Dirac equation have been carried out. Solvent effects have been taken into account using the conductor-like screening model (COSMO).²⁰ Geometry optimizations, which have been carried out at the scalar relativistic level, were followed by single-point computations including spin–orbit coupling. The Vosko–Wilk–Nusair functional²² for the local density approximation and the

gradient corrections for the exchange and correlation of Becke and Perdew,²³ respectively, i.e., the BP86 functional, have been used. The calculations were performed using the Amsterdam density functional (ADF2010.02) program package.^{21c} Triple- ζ Slater-type valence orbitals augmented by one set of polarization functions (TZP) were used for all atoms. For all elements, the basis sets were taken from the ADF/ZORA/TZP database directory. The frozen-core approximation, where the core density is obtained from four-component Dirac–Slater calculations, has been applied for all atoms. For C 1s, the 1s core electrons were frozen. The 1s/2s/2p cores were frozen respectively for Cl 2p, P 2p, and Si 2p. The U 5d valence space of the heavy element includes the 5f/6s/6p/6d/7s/7p shells (14 valence electrons). Several studies have shown that the ZORA/BP86/TZP approach reproduces the experimental geometries and ground-state properties of f-element compounds with satisfying accuracy.^{24–28} We also carried out calculations using the more extended ZORA TZ2P basis set, which contains two sets of polarization functions, to check the accuracy of the computed properties. Molecular geometry and molecular orbital (MO) plots were generated respectively by using the MOLEKEL 4.3²⁹ and ADFVIEW^{21c} programs.

The theoretical determination of EAs is reputed to be a difficult task.⁶ Computed EAs generally involve odd-electron systems where spin contamination and self-consistent-field convergence problems add to the difficulty of producing reliable results. Because available experimental EAs of molecules and complexes are largely adiabatic, the most direct theoretical method consists of calculation of the energy difference between the neutral and anionic (or cationic) forms of the complexes at their respective optimized geometries, i.e., the “ ΔE method”.

In terms of the energies E at optimized geometries, the EA and ionization energy (IE) are computed as follows:

$$EA = E(\text{neutral}) - E(\text{anion})$$

for the reduction reaction

$$IE = E(\text{cation}) - E(\text{neutral})$$

for the oxidation reaction

The ADF program that we use produces total bonding energies (TBEs) rather than total energies, so that EA is computed in our case

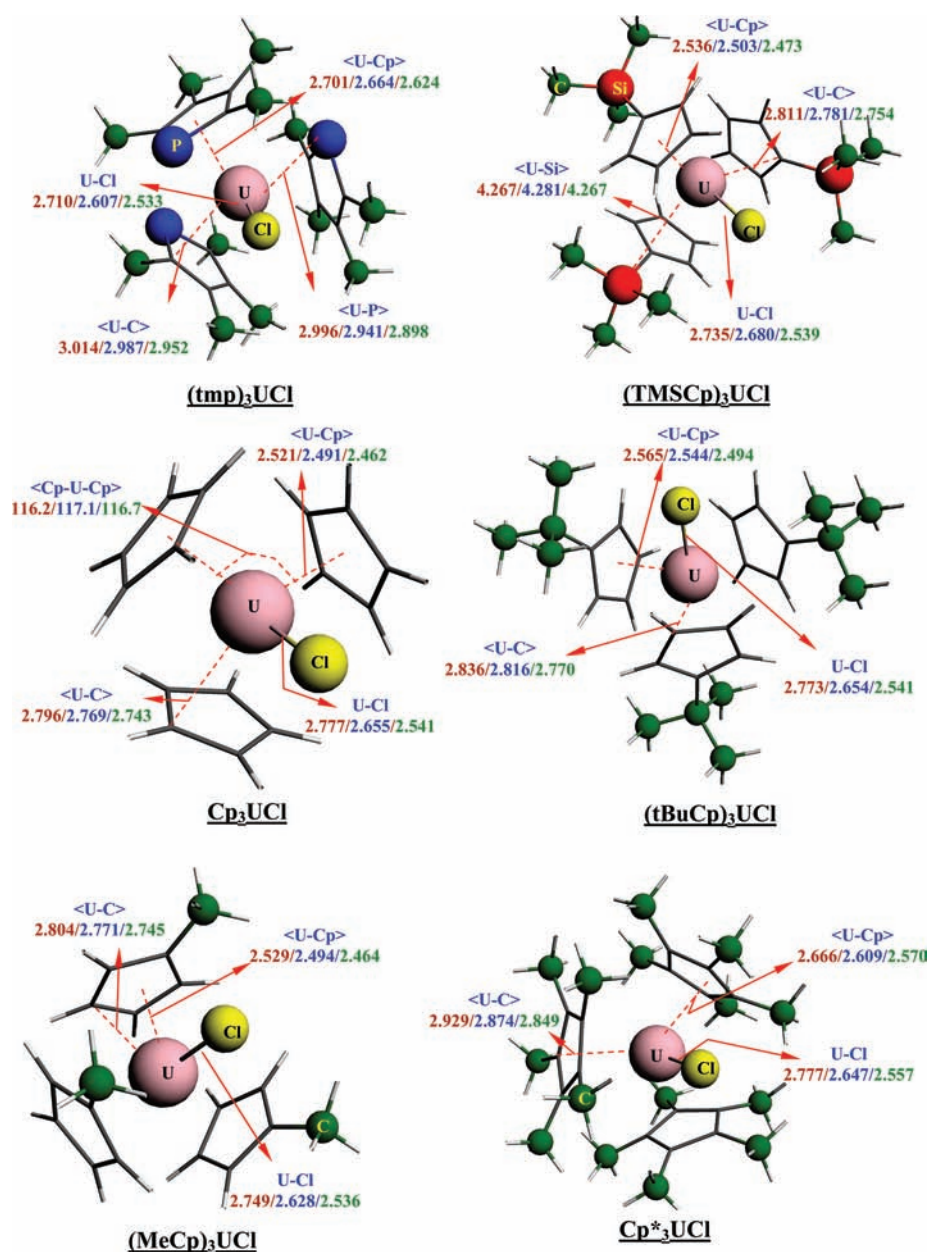


Figure 2. Optimized geometries of the uranium(III)/uranium(IV)/uranium(V) L_3UCl complexes at the TZP level in solution (THF). Hydrogen and carbon atoms of the C_5 rings are omitted for clarity.

as the $TBE(\text{neutral}) - TBE(\text{anion})$ difference for the reduction process and IE as $TBE(\text{cation}) - TBE(\text{neutral})$.

RESULTS AND DISCUSSION

Molecular Geometry Optimizations. First, the complete geometry optimizations of the neutral complexes [(tmp) $_3UCl$] (1),³⁰ [(TMSCp) $_3UCl$] (2),³¹ [Cp $_3UCl$] (3),³² [(tBuCp) $_3UCl$] (4),³³ [(MeCp) $_3UCl$] (5),³³ and [Cp* $_3UCl$] (6)³⁴ and their anionic and cationic forms were carried out in the gas phase, at the spin-unrestricted level of theory. We considered the highest spin state of all species, i.e., a triplet state ($5f^2$) for the neutral uranium(IV) compounds, a quartet state ($5f^3$) for the anionic uranium(III) ones, and a doublet state ($5f^1$) for the cationic uranium(V) ones. Calculations confirming their triplet ground state have also been carried out considering uranium(IV) complexes in their singlet state. All compounds have been taken in C_1 symmetry, except 3, which exhibits C_5 symmetry.

Then, the geometries were further reoptimized in solution [tetrahydrofuran (THF) solvent] using the COSMO approach. The nondefault Delley type of cavity was used, with the solvent being considered with its dielectric constant of 7.58 and radius of 3.18 Å.

Finally, single-point variational calculations using the previously optimized geometries to compute the spin-orbit coupling^{21b,35} contributions to the energies, in both the gas phase and solution, have been carried out. In our case of open-shell systems, the recommended noncollinear approximation^{35b} was used.

In Table 1 are listed the most relevant computed geometrical parameters, i.e., metal–ligand distances and bond angles for the three uranium(III), uranium(IV), and uranium(V) species in the gas phase as well as in solution at the ZORA/BP86/TZP level [optimized structures and coordinates in the Supporting Information (SI)].

Table 2. EAs (eV) of the Uranium(IV) L_3 UCl Complexes at the TZP (and TZ2P) Levels in the Gas Phase and in Solution (in Parentheses) and the Experimental Half-Wave Reduction Potentials $E_{1/2}$ (V)

	1 (tmp)	2 (TMSCp)	3 (Cp)	4 (^t BuCp)	5 (MeCp)	6 (Cp*)
TZP	1.709 (2.940)	1.623 (2.796)	1.405 (2.855)	1.371 (2.695)	1.260 (2.681)	1.149 (2.467)
TZP/SO	1.981 (3.206)	1.841 (3.019)	1.641 (3.007)	1.650 (2.964)	1.527 (2.939)	1.492 (2.811)
TZ2P	1.743 (2.873)	1.629 (2.803)	1.392 (2.847)	1.379 (2.687)	1.266 (2.671)	1.169 (2.474)
TZ2P/SO	2.013 (3.175)	1.848 (3.026)	1.650 (2.987)	1.655 (2.946)	1.536 (2.929)	1.500 (2.810)
exptl $E_{1/2}$ (V)	-1.614	-1.826	-1.875	-1.927	-1.948	

Globally, the optimized molecular geometries of the uranium(IV) complexes are in good agreement with the experimental data available, namely, those of complexes **1**, **3**, and **6**.^{30,32,34} The best agreement is observed with the optimized values in solution rather than in the gas phase. While the U–Cl distances are well reproduced by the computations for complexes **1** and **3**, the calculated value of 2.647 Å in **6** is definitely smaller than the exceptionally large, as previously pointed out,³⁴ X-ray distance of 2.900 Å. The average U–C and U–L(centroid) distances are also well reproduced because the deviations between the theoretical and experimental values do not exceed 0.05 Å, except in the case of **1** (0.08 Å deviation for U–C). The computed U–P distance and C–P–C bond angle of **1** are close to the X-ray data (2.996 vs 2.927 Å and 90.4 vs 90.1°). The computed values of the Cp–U–Cp angles (116.9–118.3°; see the SI) correspond well to the experimental data (116.7–120°), whereas the agreement obtained for the Cp–U–Cl angles is better (less than 2°).

The $U^{IV} \rightarrow U^{III}$ reduction process of the neutral complexes induces a significant increase of the calculated bond distances. For the U–Cl bond, this increase is equal to 0.11–0.13 Å for all compounds except **2** (0.05 Å), whereas for the U–L(centroid) distances, it varies from 0.02 Å in **4** to 0.06 Å in **6**. This bond lengthening is in line with variation of 0.135 Å in the radii of the U^{4+} and U^{3+} ions.³⁶ On the opposite side, the $U^{IV} \rightarrow U^V$ oxidation leads to a shortening of the metal–ligand bonds. The U–Cl distances decrease by ca. 0.1 Å in solution, as expected from variation in the radii of the U^{4+} and U^{5+} ions,³⁶ while the U–L(centroid) bonds are shortened by ca. 0.03 Å. In addition, the C–C and C–H bond lengths of the ligands and the centroid–U–centroid and centroid–U–X angles are not affected by reduction or oxidation of the neutral uranium(IV) compound because the variations do not exceed 0.02 Å for the distances and 1° for the angles.

Finally, the use of a more extended basis set, i.e., the TZ2P triple- ζ basis set, which contains two polarization functions, leads, as expected, to optimized geometries that are practically the same as those obtained with the TZP basis set (see the SI).

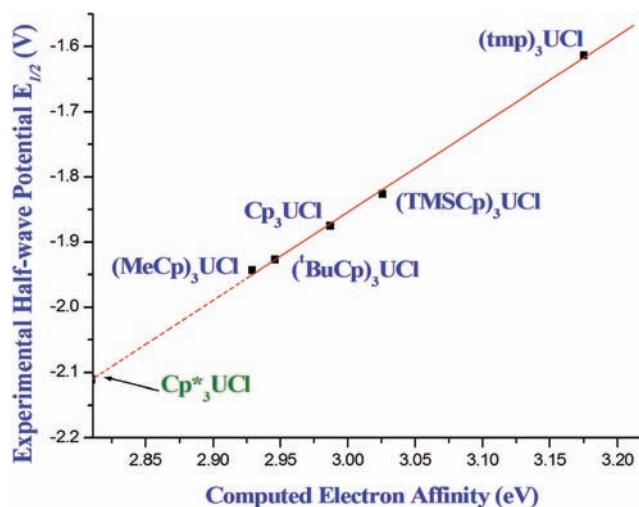
The optimized molecular geometries of the neutral uranium(IV), anionic uranium(III), and cationic uranium(V) complexes are depicted in Figure 2.

Redox Properties. First, we examine reduction of the neutral uranium(IV) complexes. In all cases, the EAs were computed according to the “ ΔE method”, that is, the difference between the TBEs of the neutral uranium(IV) and anionic uranium(III) species at their optimized geometries (the TBE values are given in the SI). In Table 2 are given the computed EAs, in the gas phase as well as in solution, for all complexes; the lines with the acronym SO correspond to the values of the EA taking into account spin–orbit coupling. In the last line of Table 2 are displayed the experimental half-wave reduction potentials in volts [$E_{1/2}$ vs $[Cp_2Fe]^{+/0}$] of the neutral uranium(IV) complexes].³⁷

We discuss first the EA values obtained in the gas phase. As expected, the computed EAs are all positive because the TBEs of the anionic species are lower than those of their neutral parents.

Spin–orbit coupling affects differently the TBEs of the neutral and anionic species, in their triplet and quartet states, respectively, with the latter complexes undergoing an energy lowering of 2.5 eV on average, whereas it is of 2.2 eV for the uranium(IV) compounds. Solvent effects and spin–orbit coupling corrections lead to significant variations of EAs. Moreover, it is interesting to note that relative ordering of the EAs of the uranium(IV) complexes in the gas phase can be changed in solution, as is the case for **3** and **4**.

A very good linear correlation is obtained between the computed EAs (in solution at the TZ2P level including the spin–orbit correction) and the experimental half-wave reduction potentials $E_{1/2}$, with the r^2 correlation coefficient of the linear regression being equal to 0.99 (Figure 3).

**Figure 3.** Correlation between the computed EAs and the experimental half-wave potentials $E_{1/2}$ for the L_3 UCl complexes in solution at the TZ2P level.

We note that neglecting spin–orbit coupling worsens dramatically the EA– $E_{1/2}$ correlation (r^2 is lower than 0.90). This result agrees with a recent DFT study, taking into account solvation effects with COSMO, which shows that spin–orbit corrections to the An^{VI}/An^V reduction potential of the actinyl complexes $[AnO_2(H_2O)_5]^{n+}$ ($An = U, Np,$ and Pu) are essential.³⁸ Finally, it is worth noting that the use of the less extended TZP basis set slightly worsens the correlation between EA and $E_{1/2}$, with the r^2 factor being equal to 0.98.

This good correlation permits one to estimate the half-wave reduction potential of **6**. On the basis of the linear regression of Figure 3 and the computed EA of **6**, i.e., $EA = 4.37 + 0.74 E_{1/2}$

Table 3. Computed SOMO and LUMO Energies of the Uranium(III) and Uranium(IV) Complexes at the TZP level and Highest Occupied Spinors of Uranium(III) Energies and Lowest Unoccupied Spinors of Uranium(IV) Energies at the TZP and TZ2P Levels (Computed Values in THF Solution in Parentheses)

complex	scalar ZORA calculations		spin-orbit ZORA calculations ^a			
	U ^{III} SOMO energy (eV)	U ^{IV} LUMO energy (eV)	U ^{III} HOS energy (eV)		U ^{IV} LUS energy (eV)	
	TZP	TZP	TZP	TZ2P	TZP	TZ2P
(tmp) ₃ UCl	0.444 (−1.995)	−3.582 (−3.639)	0.244 (−2.169)	0.229 (−2.179)	−3.610 (−3.628)	−3.624 (−3.553)
(TMSCp) ₃ UCl	0.682 (−1.709)	−3.592 (−3.627)	0.531 (−1.835)	0.458 (−1.880)	−3.586 (−3.621)	−3.650 (−3.671)
Cp ₃ UCl	1.235 (−1.619)	−3.619 (−3.717)	1.138 (−1.884)	1.031 (−1.938)	−3.638 (−3.798)	−3.730 (−3.837)
(^t BuCp) ₃ UCl	1.028 (−1.515)	−3.381 (−3.493)	0.878 (−1.639)	0.812 (−1.688)	−3.412 (−3.517)	−3.481 (−3.566)
(MeCp) ₃ UCl	1.266 (−1.479)	−3.432 (−3.521)	1.180 (−1.551)	1.111 (−1.605)	−3.457 (−3.598)	−3.521 (−3.584)
Cp* ₃ UCl	1.243 (−1.246)	−3.027 (−3.216)	0.953 (−1.509)	0.907 (−1.520)	−3.059 (−3.270)	−3.101 (−3.289)

^aHOS = highest occupied spinor; LUS = lowest unoccupied spinor.

and EA(Cp*₃UCl) = 2.81 eV, we obtained $E_{1/2}(\text{Cp}^*_3\text{UCl}) = -2.11$ V. Such a $E_{1/2}$ value makes this compound difficult to reduce electrochemically. Experimentally, no sign of decomposition of **6** was observed at 60 °C over a period of 3 days, while the bromide analogue [Cp*₃UBr] was immediately thermally transformed into the uranium(III) complex [Cp*₂UBr] with elimination of (C₅Me₅)₂, following a so-called sterically induced reduction reaction.³⁴

The influence of the nature of the L ligand on the EAs of the L₃UCl complexes **1–6** is clearly related to electronic effects: strong electron donor ligands lead to low EA complexes. By comparison with **3**, the larger EA and $E_{1/2}$ of **2** indicate the weaker electron-donating capacity of TMSCp relatively to Cp.¹¹ Complexes **4–6**, which bear the more electron-donating ligands MeCp, ^tBuCp, and Cp*, exhibit smaller EA and $E_{1/2}$ values. As was previously observed in the series of [L₂U(BH₄)₂] complexes,¹⁶ L₃UCl complexes with L = Cp* or tmp have the lowest and highest EAs, respectively. The fact that the phospholyl ligand is much less electron-donating than the cyclopentadienyl group was demonstrated considering the reduction potentials of [Cp₂Fe] and [(C₅H₄P)₂Fe], −2.93 and −2.15 V vs SCE, respectively,³⁹ and was also observed in the distinct coordination chemistry of tmp complexes and their Cp and Cp* counterparts.⁴⁰ As given by the Hammett constants,⁴¹ the electron-donating abilities of the L ligands should follow the order tmp < TMSCp < Cp < ^tBuCp < MeCp < Cp*, which correlates well with the EAs.

In order to investigate the change undergone by the electronic structures upon reduction, the MO diagrams of both neutral L₃UCl complexes and the corresponding anions are now considered. The computed energies of frontier orbitals, the singly occupied molecular orbital (SOMO) of uranium(III) complexes and the lowest unoccupied molecular orbital (LUMOs) of uranium(IV) ones, in the gas phase and in THF solution, as obtained in the scalar relativistic case, as well as spinor energies when taking into account the spin-orbit coupling, are given in Table 3. The effect of spin-orbit coupling on one-electron energies is more pronounced for the uranium(III) species than for the neutral uranium(IV) complexes. Moreover, the spinor energies vary in the same way as the frontier orbital energies.

Reduction of the uranium(IV) species could be schematically seen as a single-electron capture by the uranium ion that passes from electron configuration 5f² to 5f³; the electron captured by the neutral uranium(IV) complex should go in its LUMO, whereas it will be described by the highest SOMO of the reduced uranium(III) compound.

In the gas phase, the SOMO energies of the anionic uranium(III) complexes are positive and these energies become negative in THF because of the stabilizing effect of the solvent. On the other hand, the energies of the LUMO of the uranium(IV) complexes are all negative, thus revealing the capacity of these species to undergo a reduction process. Variation of the SOMO energies of the uranium(III) species is similar to that of the EAs or the reduction potentials, with the lowest SOMO corresponding to the highest EA. The energies of the highest SOMO decrease according to the order Cp* > ^tBuCp > MeCp > Cp > TMSCp > tmp, and a good linear correlation is found between the uranium(III) SOMO energies and the experimental potentials $E_{1/2}$ ($r^2 = 0.99$; Figure 4).

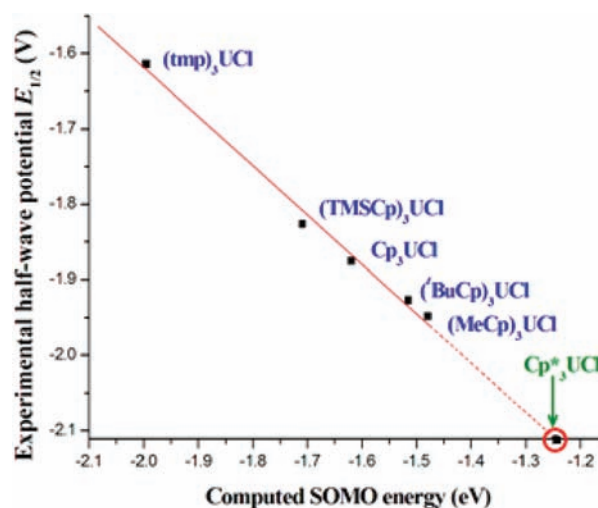


Figure 4. SOMO uranium(III) energies computed at the scalar ZORA/BP86/TZP level in THF versus experimental half-wave reduction potentials.

According to this correlation, the extrapolated value of $E_{1/2}$ for **6**, corresponding to a SOMO energy of −1.246 eV, is −2.1 V, in accordance with that calculated from the EA vs $E_{1/2}$ correlation (Figure 3).

Figure 5 shows three frontier orbitals of the neutral uranium(IV) complexes, namely, two SOMOs, each containing a single 5f electron and the empty LUMO. Percentages (6d/5f/U/L₃) indicate the weight of the 6d and 5f metal orbitals as well as those of uranium and substituted aromatic L₃ ligands in the MOs (more detailed frontier orbital diagrams are given in the SI).

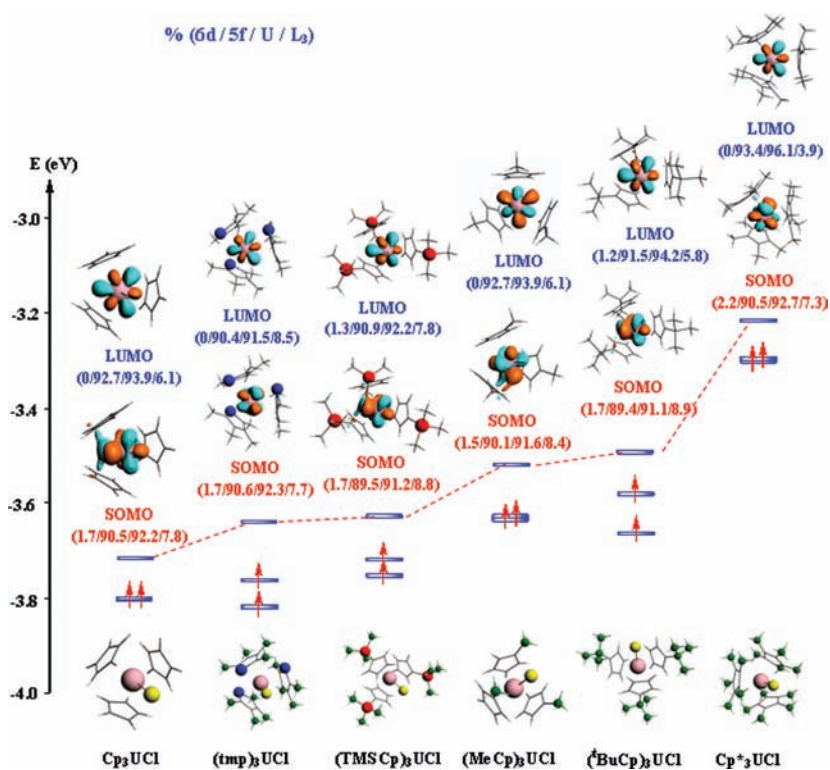


Figure 5. Frontier orbital diagrams of the uranium(IV) complexes (scalar ZORA/BP86/TZP computations in THF).

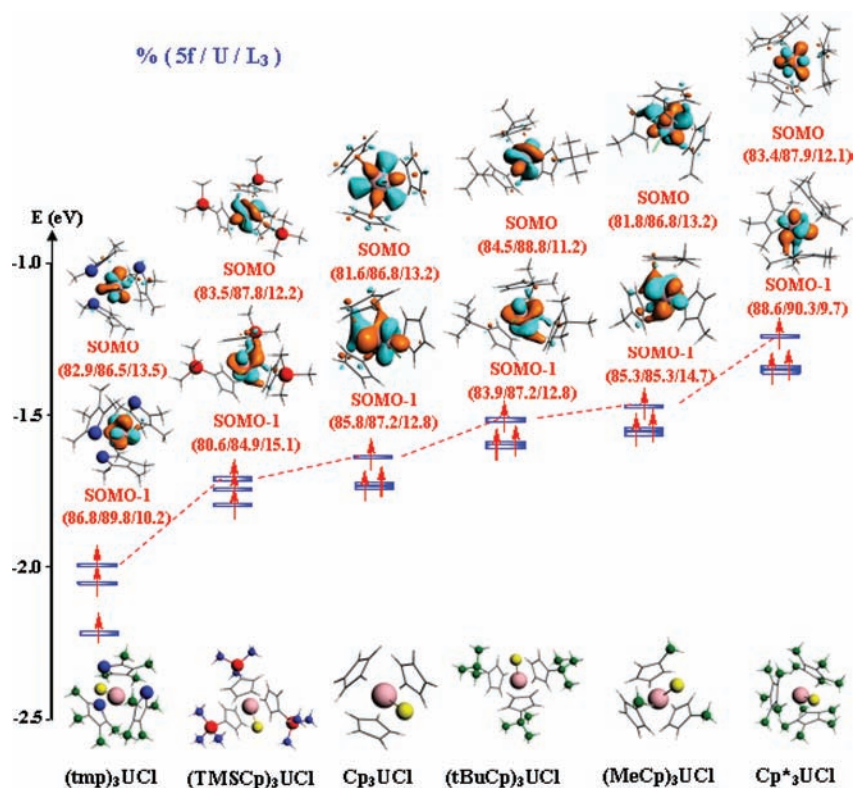


Figure 6. Frontier orbital diagrams of the uranium(III) complexes (scalar ZORA/BP86/TZP computations in THF).

These frontier orbitals are mainly U 5f orbitals with a rather substantial contribution of the L aromatic ligands; the latter contribution is the smallest for $[\text{Cp}^*_3\text{UCl}]$, whereas the contribution of chlorine to this complex is 0. The Cp^*_3 ligands, which exhibit the highest electron-donating ability,

induce an increase of the LUMO energy, leading to a decrease of the EA of the corresponding complex, whereas the more electron-attracting $(\text{tmp})_3$ ligands induce a lowering of the LUMO energy, thus making the species easier to reduce. With the exception of 3, the LUMO energies follow the same order

Table 4. TBE of Cationic Uranium(V) Complexes at the ZORA/BP86/TZP Level in the Gas Phase and in a THF Solution (in Parentheses) and Energy Differences between the Uranium(IV) and Uranium(V) Compounds [$IE = \Delta(TBE) = TBE(\text{cation}) - TBE(\text{neutral})$]

cation	Cp ₃ UCl	(MeCp) ₃ UCl	(^t BuCp) ₃ UCl	(TMSCp) ₃ UCl	(tmp) ₃ UCl	Cp* ₃ UCl
TZP	-193.087 (-194.851)	-242.425 (-244.074)	-388.021 (-389.515)	-377.931 (-379.436)	-365.001 (-366.304)	-436.956 (-438.244)
TZP/SO	-195.347 (-197.136)	-244.574 (-246.287)	-390.262 (-391.665)	-380.147 (-381.600)	-367.177 (-368.523)	-439.191 (-440.480)
$\Delta(TBE)$	5.506 (5.155)	6.123 (5.523)	6.514 (5.323)	6.561 (5.443)	6.557 (5.203)	5.239 (4.958)

Table 5. MPA and N–M Bond Orders of L₃UCl Complexes (Scalar ZORA/BP86/TZP Computations in THF)

complex	complex charge	spin population	MPA			N–M bond orders	
			net charges			U–L ^a	U–Cl
			U ^q	L ₃	Cl		
(tmp) ₃ UCl	1–	2.95	+0.942	–1.397	–0.545	1.325	0.841
	0	2.26	+0.783	–0.374	–0.409	1.486	1.064
	1+	1.37	+0.584	+0.682	–0.266	1.723	1.284
(TMSCp) ₃ UCl	1–	2.92	+0.886	–1.296	–0.590	1.289	0.785
	0	2.20	+0.740	–0.290	–0.450	1.424	1.032
	1+	1.29	+0.589	+0.701	–0.289	1.651	1.304
Cp ₃ UCl	1–	2.92	+0.972	–1.323	–0.649	1.320	0.749
	0	2.19	+0.844	–0.347	–0.497	1.454	1.002
	1+	1.29	+0.677	+0.625	–0.302	1.667	1.324
(^t BuCp) ₃ UCl	1–	2.96	+0.998	–1.391	–0.607	1.257	0.748
	0	2.22	+0.844	–0.369	–0.476	1.429	1.025
	1+	1.31	+0.680	+0.620	–0.299	1.635	1.286
(MeCp) ₃ UCl	1–	2.93	+0.935	–1.317	–0.618	1.295	0.777
	0	2.18	+0.777	–0.303	–0.474	1.441	1.027
	1+	1.28	+0.579	+0.727	–0.306	1.656	1.301
Cp* ₃ UCl	1–	3.07	+1.183	–1.569	–0.615	1.105	0.720
	0	2.30	+1.115	–0.638	–0.477	1.353	0.963
	1+	1.43	+1.059	+0.269	–0.328	1.583	1.205

^aThe N–M bond order of U–L is computed as the sum of the five U–X (X = C or P) bond orders of the ring.

as the EAs: tmp < TMSCp < MeCp < ^tBuCp < Cp*. This result is similar to that obtained from calculations on bicyclopentadienyl- and phospholyluranium(IV) borohydride complexes.¹⁶

Moreover, it is possible to correlate quantitatively the EAs of the complexes to the electron-donating ability of the ligands, using their σ Hammett coefficients.⁴¹ Indeed, a rather good correlation (with $r^2 = 0.953$) is found between the EAs and the latter coefficients considering four complexes, 3, 2, 5, and 4, for which the values of the Hammett constants are available.

All singly occupied frontier orbitals of the anionic uranium(III) species displayed in Figure 6 exhibit, like their neutral parents, a major 5f metallic character with a minor contribution of the aromatic L ligands (12.5% on average). In this figure, one notes that 1 and 6 exhibit respectively the SOMO of lowest (–1.995 eV) and highest (–1.246 eV) energy. As was already seen in Table 3, variation of the SOMO energies follows well that of the EAs, with the highest SOMO corresponding to the lowest EA; this correlation between the SOMO energies and experimental half-wave potentials $-E_{1/2}$ (or EAs) is better ($r^2 = 0.996$) than that between the LUMOs of the uranium(IV) species and $-E_{1/2}$.

Now, we focus on oxidation of the L₃UCl complexes; the calculated TBEs of the cationic uranium(V) (5f¹) complexes are compared with those of the neutral uranium(IV) species in Table 4. TZP/SO values include spin–orbit corrections (the frontier orbital diagrams of the uranium(V) species are given in the SI).

The value of $\Delta(TBE)$, that is the adiabatic IE of the uranium(IV) complexes, is very high, nearly twice the EA of the uranium(III) species, making the stability of the corresponding cationic uranium(V) complexes questionable. In fact, this

theoretical result is in line with the electrochemical study of the (RCp)₃UCl compounds, which revealed that the one-electron transfer is rapidly followed by a disproportionation reaction, regenerating the uranium(IV) complex.^{37b}

Classification of the uranium(V) complexes by decreasing the order of their IEs in solution, 5 > 2 > 4 > 1 > 3 > 6, shows that 5 is the most difficult to oxidize.

In order to reveal other aspects of metal-to-ligand bonding, three electron population analyses have been carried out, i.e., the Mulliken population analysis (MPA), the Nalewajski and Mrozek (N–M) bond index approach,⁴² and the Hirshfeld charge analysis.⁴³ Although it has known drawbacks, MPA may indicate roughly the major charge transfers and bonding interactions when homologous series of molecules are compared. MPA metal spin populations (difference between the total α and β electronic populations of the metal), net charges carried by the metal and ligands, and bond orders are consigned in Table 5. In this table, 1–, 0, and 1+ indicate respectively the anionic uranium(III), the neutral uranium(IV), and the cationic uranium(V) species.

The L₃ net charge is the sum of the three aromatic L charges and not only that of the atom connected to uranium. MPA illustrates well the ligand-to-metal donation, highlighted at the same time by the metallic net charge, which is largely smaller than its oxidation state, and by the weak negative charges carried by the L anionic ligands. The L ligand-to-metal donation, which is indicated by the L₃ net charge, increases with the oxidation state of the metal; indeed, a greater electron density is transferred to the metal when passing from

Table 6. Hirshfeld Charges of Chlorine, Uranium, and L₃ of Uranium(III)/Uranium(IV)/Uranium(V) Complexes in Solution (Scalar ZORA/BP86/TZP)

ligand/fragment	chlorine	uranium	L ₃
tmp	-0.2812/-0.1793/-0.0845	0.4711/0.5392/0.5541	-1.1893/-0.3592/0.5304
TMSCp	-0.3175/-0.1920/-0.0883	0.5484/0.6684/0.6864	-1.2302/-0.4555/0.4019
Cp	-0.4156/-0.2858/-0.1270	0.5384/0.6542/0.7040	-1.1232/-0.3684/0.4231
^t BuCp	-0.3324/-0.2291/-0.0905	0.5470/0.6567/0.6828	-1.2143/-0.4289/0.4076
MeCp	-0.3267/-0.2104/-0.0951	0.5365/0.6437/0.6828	-1.2097/-0.4334/0.4122
Cp*	-0.3006/-0.1985/-0.0967	0.5393/0.6243/0.6408	-1.2375/-0.4250/0.4559

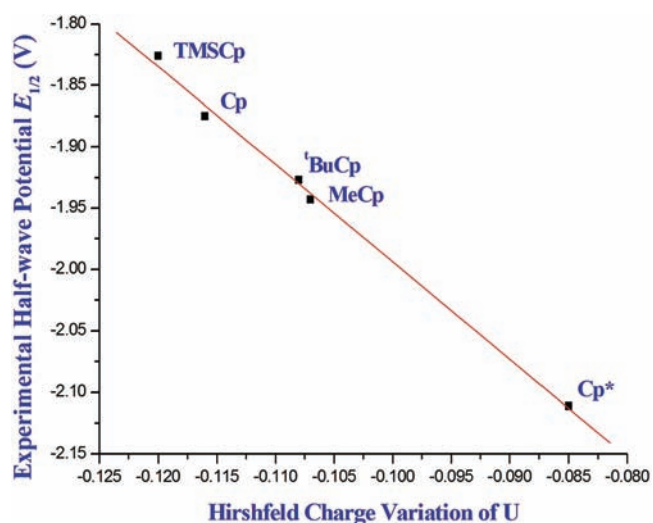
uranium(III) to uranium(IV) and uranium(V) species. Interestingly, the net charges carried by the substituted aromatic ligand L₃ in the cationic uranium(V) species are largely positive (exceeding 0.62+, except for 6⁺) and could be a factor of the instability of these species.

In addition, it is worth noting that the metal spin population values are only slightly larger than 2 for the neutral 5f² uranium(IV) species, larger than 1 for the cationic 5f¹ uranium(V), and smaller than 3 for the anionic 5f³ uranium(III) ones, except for 6, where it is 3.07, so that practically no spin delocalization on the ligands occurs. Indeed, the computed metal spin populations are equal to 2.92 and 2.96 for 2⁻ and 4⁻, respectively, with a minor spin density on the L ligand, while those of the corresponding uranium(IV) species in solution are 2.20 and 2.22, respectively. The solvent effect on the MPA net charges is not negligible (numerical values are given in the SI). Indeed, the uranium net charge is affected by the solvent, particularly for the reduced anionic uranium(III) species; its increase extends from 0.087+ to 0.017+, except for the Cp*₃UCl complex, for which a charge decrease of 0.065 is observed. Moreover, the solvent generates a lowering of the metallic charges of about 0.025 for the cationic species. Concomitantly, the net charges of the L ligand undergo a slight increase in the presence of solvent (from 0.010 to 0.043), whereas the permethylated cyclopentadienyl group C₅Me₅ charge decreases by 0.170; moreover, a significant diminution is observed for the net charges of the chloride ligand (0.080 average) for the different species. Finally, the metal spin populations computed in the solvent are practically equal to those obtained for isolated molecules (the variation does not exceed 0.01).

N–M bond orders are useful tools to study the electronic structure of organometallic complexes.⁴⁴ As expected, the value for the U–L bond is much higher than that for the U–Cl single bond. All values increase with the oxidation state of the metal. We note that the solvent leads to an appreciable decrease of the N–M bond order for all U–Cl bonds, particularly for the uranium(III) and uranium(IV) species by average amounts of 0.06–0.16 and 0.05–0.13, respectively, in agreement with variation of the bond lengths due to the solvent (Table 1). On the contrary, a very slight increase in these indices is observed for the U–L distances, except for 1. It is also worth noting that the stretching frequencies of the U–Cl bonds increase with the oxidation state of the metal, in agreement with the increase of the N–M bond order. For example, the values of 239, 277, and 309 cm⁻¹ were obtained for the [(tmp)₃UCl]^q complexes with q = 1–, 0, and 1+, respectively.

An alternative method to Mulliken charges is provided by Hirshfeld's analysis (HA), which is supposed to give more realistic net charges than MPA. In Table 6 are given the Hirshfeld charges of uranium and chlorine atoms and of the L₃ fragment respectively of the anionic, neutral, and cationic L₃UCl species, computed at the TZP level in solution.

For a given complex, in agreement with MPA, we observe the diminution of the net charges of the ligands, indicating the increase of electron donation to the metal center when the uranium oxidation state increases. In the same way, it is worth noting that the net charges of the aromatic L ligands, as given by MPA and HA, become positive for the uranium(V) species. More naturally and contrarily to MPA, the HA net charges of the central metal do not decrease with its oxidation state but increase slightly. Finally, it is worth noting that variations of the Hirschfeld uranium charges of the different complexes, excluding the particular L = tmp case, when passing from the uranium(IV) to uranium(III) complexes correlate very well with the half-wave reduction potentials of these complexes, with the r² correlation coefficient being equal to 0.996 (Figure 7). Such a good correlation is not obtained with MPA charges.

**Figure 7.** Uranium Hirshfeld charge variation following the uranium(IV)/uranium(III) reduction versus experimental half-wave potentials (scalar ZORA/BP86/TZP computations in THF).

Indeed, the differences between the uranium Hirshfeld charges in the uranium(IV) and uranium(III) species (Table 6) are the following: 0.085, 0.107, 0.109, 0.116, and 0.120 respectively for L = Cp*, MeCp, ^tBuCp, Cp, and TMSCp. They are in reverse order of the donating abilities of the ligand. More electron-donating ligands are at the origin of the smallest increases of the uranium charge after electron capture by the neutral uranium(IV) species. This result is consistent with the fact that a neutral uranium(IV) complex bearing a strong electron-donating ligand is more difficult to reduce electrochemically.

CONCLUSION

The EAs of a series of tricyclopentadienyl- and phospholyluranium(IV) chloride complexes L₃UCl (L = Cp, TMSCp,

^tBuCp, MeCp, tmp, and Cp*) have been computed using relativistic ZORA/BP86 computations including spin-orbit coupling, with solvent effects being taken into account using the COSMO approach. A very good linear correlation ($r^2 = 0.99$) was found between the computed EAs and experimental half-wave reduction potentials $E_{1/2}$, thus confirming the reliability of the method chosen for the study of the reduction of such complexes. Our study brings to light the importance of spin-orbit coupling and solvent effects and the use of a large atomic basis set in order to achieve a good agreement between theory and experiment. In addition, this study allowed estimation of the half-wave reduction potential of the Cp*₃UCl complex (not measured to date).

Moreover, MO diagrams and population analyses permitted one to understand the evolution of EAs with the nature of the aromatic L ligand, especially with its electron-donating capacity. Indeed, the EAs decrease with the electron-donating strength of L according to tmp < TMSCp < Cp < ^tBuCp < MeCp < Cp*. A rather good correlation exists between the Hammett constants of the ligands and the EAs of the complexes. Finally, an excellent correlation ($r^2 = 0.996$) between the Hirshfeld charge variation of the uranium atom following the uranium(IV)/uranium(III) process and the half-wave reduction potentials has been found, with the more electron-donating ligand leading to the smallest increase of the uranium charge after electron capture by the neutral uranium(IV) species.

Considering the oxidation reaction of the neutral uranium(IV) complexes, the computed energies of the cationic species reveal the unstable character of the uranium(V) complexes in agreement with experimental data resulting from an electrochemical study. This instability is illustrated by the very low values of LUMO of the [L₃UCl]⁺ species, with the latter ones being able to readily undergo a reduction process.

■ ASSOCIATED CONTENT

Supporting Information

Optimized coordinates of L₃UCl complexes at the ZORA/BP/TZP level in the gas phase, population analyses, TBEs of neutral uranium(IV) and anionic uranium(III) complexes, and frontier orbital diagrams of the cationic uranium(V) species of the L₃UCl complexes. This material is available free of charge via the Internet at <http://pubs.acs.org>.

■ AUTHOR INFORMATION

Corresponding Author

*E-mail: abdou.boucekkine@univ-rennes1.fr.

Notes

The authors declare no competing financial interest.

■ ACKNOWLEDGMENTS

The authors are grateful to GENCI-IDRIS and GENCI-CINES for allocation of computing time (Grant 2011-080649).

■ REFERENCES

- (1) Takats, J. In *Fundamental and technological aspects of the organo-f-elements*; Marks, T. J., Fragala, I. L., Eds.; D. Reidel: Dordrecht, The Netherlands, 1985.
- (2) Edelman, F. In *Comprehensive organometallic chemistry*; Abel, E. W., Stone, F. G. A., Wilkinson, G., Eds.; Pergamon: Oxford, U.K., 1995; Vol. 4, Chapter 2, p 11.
- (3) Burns, C. J.; Eisen, M. S. In *The chemistry of the actinides and transactinides elements*, 3rd ed.; Morss, L. R., Edelstein, N. M., Fuger, F., Eds.; Springer: Dordrecht, The Netherlands, 2006; Vol. 5, p 2799.

- (4) Evans, W. J.; Kozimor, S. A. *Coord. Chem. Rev.* **2006**, *250*, 911.
- (5) (a) Ephritikhine, M. *Dalton Trans.* **2006**, 2501. (b) Ephritikhine, M. *Actual. Chim.* **2008**, 322, II.
- (6) Rienstra-Kiracofe, J. C.; Tschumper, G. S.; Schaefer, H. F.; Nandi, S.; Ellison, G. B. *Chem. Rev.* **2002**, *102*, 231.
- (7) Schelter, E. J.; Yang, P.; Scott, B. L.; Thompson, J. D.; Martin, R. L.; Hay, P. J.; Morris, D. E.; Kiplinger, J. L. *Inorg. Chem.* **2007**, *46*, 7477.
- (8) (a) Thomson, R. K.; Scott, B. L.; Morris, D. E.; Kiplinger, J. L. *Chimie* **2010**, *13*, 790. (b) Graves, C. R.; Vaughn, A. E.; Schelter, E. J.; Scott, B. L.; Thompson, J. D.; Morris, D. E.; Kiplinger, J. L. *Inorg. Chem.* **2008**, *47*, 11879. (c) Graves, C. R.; Yang, P.; Kozimor, S. A.; Vaughn, A. E.; Clark, D. L.; Conradson, S. D.; Schelter, E. J.; Scott, B. L.; Thompson, J. D.; Hay, P. J.; Morris, D. E.; Kiplinger, J. L. *J. Am. Chem. Soc.* **2008**, *130*, 5272. (d) Jantunen, K. C.; Burns, C. J.; Castro-Rodriguez, I.; Da Re, R. E.; Golden, J. T.; Morris, D. E.; Scott, B. L.; Taw, F. L.; Kiplinger, J. L. *Organometallics* **2004**, *23*, 4682. (e) Morris, D. E.; Da Re, R. E.; Jantunen, K. C.; Castro-Rodriguez, I.; Kiplinger, J. L. *Organometallics* **2004**, *23*, 5142. (f) Kiplinger, J. L.; Morris, D. E.; Scott, B. L.; Burns, C. J. *Organometallics* **2002**, *21*, 3073.
- (9) Finke, R. G.; Gaughan, G.; Voegeli, R. J. *Organomet. Chem.* **1982**, *229*, 179.
- (10) Mugnier, Y.; Dormond, A.; Laviron, E. *J. Chem. Soc., Chem. Commun.* **1982**, 257.
- (11) Sonnenberger, D. C.; Gaudiello, J. G. *Inorg. Chem.* **1988**, *27*, 2747.
- (12) Ossola, F.; Zanella, P.; Ugo, P.; Seeber, R. *Inorg. Chim. Acta* **1988**, *147*, 123.
- (13) (a) Hauchard, D.; Cassir, M.; Chivot, J.; Ephritikhine, M. J. *Electroanal. Chem.* **1991**, *313*, 227. (b) Hauchard, D.; Cassir, M.; Chivot, J.; Baudry, D.; Ephritikhine, M. J. *Electroanal. Chem.* **1993**, *347*, 399.
- (14) Schnabel, R. C.; Scott, B. L.; Smith, W. H.; Burns, C. J. *J. Organomet. Chem.* **1999**, *591*, 14.
- (15) Elkechai, A.; Meskaldji, S.; Boucekkine, A.; Belkhiri, L.; Bouchet, D.; Amarouche, M.; Clappe, C.; Hauchard, D.; Ephritikhine, M. J. *Mol. Struct. (THEOCHEM)* **2010**, *954*, 115.
- (16) Elkechai, A.; Boucekkine, A.; Belkhiri, L.; Hauchard, D.; Clappe, C.; Ephritikhine, M. C. R. *Chimie* **2010**, *13*, 860.
- (17) Elkechai, A.; Boucekkine, A.; Belkhiri, L.; Amarouche, M.; Clappe, C.; Hauchard, D.; Ephritikhine, M. *Dalton Trans.* **2009**, 2843.
- (18) (a) Hohenberg, P.; Kohn, W. *Phys. Rev.* **1964**, *136*, B864. (b) Kohn, W.; Sham, L. J. *Phys. Rev.* **1965**, *140*, A1133. (c) Parr, R. G.; Yang, W. *Density functional theory of atoms and molecules*; Oxford University Press: Oxford, U.K., 1989.
- (19) (a) van Lenthe, E.; Baerends, E. J.; Snijders, J. G. *J. Chem. Phys.* **1993**, *99*, 4597. (b) van Lenthe, E.; Baerends, E. J.; Snijders, J. G. *J. Chem. Phys.* **1994**, *101*, 9783. (c) van Lenthe, E.; Ehlers, A.; Baerends, E. J. *J. Chem. Phys.* **1999**, *110*, 8943.
- (20) (a) Klamt, A.; Schürmann, G. *J. Chem. Soc., Perkin Trans.* **1993**, *2*, 799. (b) Klamt, A. *J. Phys. Chem.* **1995**, *99*, 2224. (c) Klamt, A.; Jones, V. *J. Chem. Phys.* **1996**, *105*, 9972. (d) Klamt, A.; Jones, V.; Bürger, T.; Lohrenz, J. C. *J. Phys. Chem. A* **1998**, *102*, 5074. (e) Delley, B. *Mol. Simul.* **2006**, *32*, 117. (f) Klamt, A. *COSMO-RS from quantum chemistry to fluid phase thermodynamics and drug design*; Elsevier: Amsterdam, The Netherlands, 2005; ISBN 0-444-51994-7.
- (21) (a) Fonseca, G. C.; Snijders, J. G.; te Velde, G.; Baerends, E. J. *Theor. Chem. Acc.* **1998**, *99*, 391. (b) te Velde, G.; Bickelhaupt, F. M.; van Gisbergen, S. A. J.; Fonseca, G. C.; Baerends, E. J.; Snijders, J. G.; Ziegler, T. *J. Comput. Chem.* **2001**, *931*. (c) *ADF2008.01, SCM, Theoretical Chemistry*; Vrije University: Amsterdam, The Netherlands, <http://www.sm.com>.
- (22) Vosko, S. D.; Wilk, L.; Nusair, M. *Can. J. Chem.* **1990**, *58*, 1200.
- (23) (a) Becke, A. D. *J. Chem. Phys.* **1986**, *84*, 4524. (b) Becke, A. D. *Phys. Rev. A* **1988**, *38*, 3098. (c) Perdew, J. P. *Phys. Rev. B* **1986**, *33*, 8822. (d) Perdew, J. P. *Phys. Rev. B* **1986**, *34*, 7406. (e) Perdew, J. P.; Wang, Y. *Phys. Rev. B* **1992**, *45*, 13244.
- (24) Ricciardi, G.; Rosa, A.; Baerends, E. J.; van Gisbergen, S. A. J. *J. Am. Chem. Soc.* **2002**, *124*, 1233.

- (25) (a) Kaltsoyannis, N. *Chem. Soc. Rev.* **2003**, 32, 9. (b) Shamov, G. A.; Schreckenbach, G. J. *Phys. Chem. A* **2005**, 109, 10961.
- (26) Roger, M.; Belkhiri, L.; Thuéry, P.; Arliguie, T.; Fourmigué, M.; Boucekkine, A.; Ephritikhine, M. *Organometallics* **2005**, 24, 4940.
- (27) Belkhiri, L.; Lissilour, R.; Boucekkine, A. *J. Mol. Struct. (THEOCHEM)* **2005**, 757, 155.
- (28) Benyahia, M.; Belkhiri, L.; Boucekkine, A. *J. Mol. Struct. (THEOCHEM)* **2006**, 777, 61.
- (29) Flükiger, P.; Lüthi, H. P.; Portmann, S.; Weber, J. *MOLEKEL* 4.3; 2000–2002, Swiss Center for Scientific Research: Manno, Switzerland.
- (30) Gradoz, P.; Boisson, C.; Baudry, D.; Lance, M.; Nierlich, M.; Vigner, J.; Ephritikhine, M. *J. Chem. Soc., Chem. Commun.* **1992**, 1720.
- (31) Brennan, J. G.; Andersen, R. A.; Zalkin, A. *Inorg. Chem.* **1986**, 25, 1756.
- (32) Reynolds, L. T.; Wilkinson, G. J. *Inorg. Nucl. Chem.* **1956**, 2, 246.
- (33) Dormond, A.; Duval Huet, C.; Tirouflet, J. *J. Organomet. Chem.* **1981**, 209, 341.
- (34) Evans, W. J.; Nyce, G. W.; Johnston, M. A.; Ziller, J. W. *J. Am. Chem. Soc.* **2000**, 122, 12019.
- (35) (a) van Lenthe, E.; Snijders, J. G.; Baerends, E. J. *J. Chem. Phys.* **1996**, 105, 6505. (b) van Wüllen, C. *J. Comput. Chem.* **2002**, 23, 779.
- (36) Shannon, R. D. *Acta Crystallogr., Sect. A* **1976**, 32, 751.
- (37) (a) Clappe, C.; Leveugle, D.; Hauchard, D.; Durand, G. *J. Electroanal. Chem.* **1998**, 448, 95. (b) Clappe, C. Thèse de Doctorat, Université Paris VI, Paris, France, 1997.
- (38) Shamov, G. A.; Schreckenbach, G. J. *Phys. Chem. A* **2005**, 109, 10961.
- (39) Lemoine, P.; Gross, M.; Braunstein, P.; Mathey, F.; Deschamps, B.; Nelson, J. H. *Organometallics* **1984**, 3, 1303.
- (40) (a) Gradoz, P.; Baudry, D.; Ephritikhine, M.; Nief, F.; Mathey, F. *Dalton Trans.* **1992**, 3047. (b) Gradoz, P.; Baudry, D.; Ephritikhine, M.; Lance, M.; Nierlich, M.; Vigner, J. *J. Organomet. Chem.* **1994**, 466, 107.
- (41) (a) Hammett, L. P. *J. Am. Chem. Soc.* **1937**, 59, 96. (b) Laurence, C.; Wojtkowiak, B. *Ann. Chim.* **1970**, 5, 163. (c) Charlton, M. *Prog. Phys. Org. Chem.* **1981**, 13, 119. (d) Hansch, C.; Leo, A.; Taft, R. W. *Chem. Rev.* **1991**, 91, 165.
- (42) Nalewajski, R. F.; Mrozek, J. *Int. J. Quantum Chem.* **1994**, 51, 187.
- (43) Hirshfeld, F. L. *Theor. Chim. Acta* **1977**, 44, 129.
- (44) (a) Fox, R. A.; Cummins, C. C. *J. Am. Chem. Soc.* **2009**, 131, 5716. (b) Diaconescu, P. L.; Arnold, P. L.; Baker, T. A.; Mindiola, D. J.; Cummins, C. C. *J. Am. Chem. Soc.* **2000**, 122, 6108. (c) Patel, D.; King, D. M.; Gardner, B. M.; McMaster, J.; Lewis, W.; Blake, A. J.; Liddle, S. T. *Chem. Commun.* **2011**, 47, 295.